Journal of Power Sources 202 (2012) 308–313

Contents lists available at SciVerse ScienceDirect

Journal of Power Sources

journal homepage: www.elsevier.com/locate/jpowsour

A contribution to the progress of high energy batteries: A metal-free, lithium-ion, silicon–sulfur battery

Jusef Hassoun[a], Junghoon Kim[b], Dong-Ju Lee[b], Hun-Gi Jung[c], Sung-Man Lee[d], Yang-Kook Sun[b,c,**], Bruno Scrosati[a,b,*]

[a] Department of Chemistry, University of Rome Sapienza, 00185 Rome, Italy
[b] Department of WCU Energy Engineering, Hanyang University, Seoul 133-791, Republic of Korea
[c] Department of Chemical Engineering, Hanyang University, Seoul 133-791, Republic of Korea
[d] Department of Advanced Materials Science and Engineering, Kangwon National University, Kangwon-Do 200-701, Republic of Korea

ARTICLE INFO

Article history:
Received 25 October 2011
Received in revised form
18 November 2011
Accepted 19 November 2011
Available online 27 November 2011

Keywords:
Sulfur
Silicon
Lithium ether electrolyte
Lithium ion battery

ABSTRACT

In this work we disclose a new, lithium metal-free, silicon–sulfur, lithium ion battery based on a high-rate sulfur–carbon composite cathode, formed by trapping sulfur in highly porous and hard carbon spherules, combined with a lithiated, silicon–carbon nanocomposite anode, separated by a glycol-based electrolyte. This 2 V battery shows an average specific capacity of 300 mAh $g^{-1}_{(S)}$, a long cycle life, an expected low cost and high safety. Due to these properties, this new battery is expected to be a very valid power source for efficient electric vehicles.

1. Introduction

Lithium batteries are the power sources of choice for the consumer electronic market and are being aggressively developed for the road transportation sector. However, it is now clear that these batteries can be truly effective for powering electric cars only if they are able to assure long driving distance in a single charge (of the order of few hundred kilometers). The present lithium battery technology is not adequate since, given that the available energy density averages around 150 Wh kg^{-1}, a battery weight exceeding any acceptable limit would be necessary to meet the driving distance goal. New batteries having energy density levels at least three times higher than the present ones are urgently needed.

Due to its theoretical high gravimetric and volumetric energy [1,2], a good candidate is the lithium–sulfur battery. Most of the early studies of this system were based on a cell configuration involving a carbon–sulfur mixture as the cathode, lithium metal as the anode, and a solution of a lithium salt in carbonate organic solvents as the electrolyte [3–8]. The performance of the battery was limited by series of issues, a major one being the uncontrolled solubility of the reaction products.

The main electrochemical process, i.e., 16 Li + $S_8 \leftrightarrows$ 8 Li_2S, proceeds throughout the formation of a series of polysulfides, Li_2S_x ($1 \leq x \leq 8$), which are highly soluble in the electrolyte medium. This reaction results in a loss of active material mass, which, in turn, causes a low utilization of the sulfur cathode and severe capacity decay upon cycling [2]. The dissolved polysulfide anions, by migration through the electrolyte, may reach the lithium metal anode, where they react and form insoluble products on the anode surface, further depressing the battery operation [9]. Moreover, S^{2-} is a very strong base and nucleophile that may readily react with the carbonate esters commonly used in the electrolyte. Another issue was the limited functionality of the carbon–sulfur electrode morphology, since the two components tend to agglomerate with resulting increase of the electrode resistance and loss of reciprocal contacts, both decreasing the cycle life and the rate capability of the electrode. Finally, a serious safety concern may arise when metal lithium is used as the anode.

These hurdles have some time cooled down the interest in the lithium–sulfur battery. However, the attention in this system rose again in the latest years due to a series of important technological breakthroughs. Optimization in the fabrication of the cathode,

* Corresponding author at: Department of Chemistry, University of Rome Sapienza, 00185 Rome, Italy.
** Corresponding author at: Department of Chemical Engineering, Hanyang University, Seoul 133-791, Republic of Korea.
E-mail addresses: yksun@hanyang.ac.kr (Y.-K. Sun), bruno.scrosati@uniroma1.it (B. Scrosati).

0378-7753/$ – see front matter © 2011 Elsevier B.V. All rights reserved.
doi:10.1016/j.jpowsour.2011.11.060

passing from simple sulfur–carbon mixtures to sulfur–carbon composites, e.g. by immobilizing sulfur in carbon pores [10], in microporous or hollow carbon spheres [11,12], or by developing polysulfide reservoirs based on porous silica embedded within the carbon–sulfur composite [13], substituting the very reactive lithium metal with more reliable tin [14] or the lithium sulfide dissolving liquid organic carbonate electrolytes with polymer electrolytes [15], proved to be successful approaches for improving the conductivity of the electrode, as well as for controlling the solubility of the discharge products.

These results consistently contributed to increase the interest in the lithium–sulfur battery; however, some residual issues still prevent the full practical implementation of this high energy battery system. Most of the recent works still rely on conventional liquid organic carbonate solution as the preferred electrolyte and on the use of lithium metal as the preferred anode material. Therefore, concern in the battery cycle life, due to the solubility of the reaction products, and in its safety, due to the reactivity of the anode, remains.

In this work we report an advanced lithium metal-free, silicon–sulfur, lithium ion battery based on a high-rate sulfur–carbon composite cathode combined with a lithiated, silicon–carbon nanocomposite anode, separated by a glycol-based electrolyte. We demonstrate that these new concepts allow to mark a step forward in the lithium–sulfur battery technology.

2. Experimental

2.1. Synthesis of HCS and HCS-S composite cathode

Mesoporous hard carbon spherules (HCS) were prepared by a hydrothermal method using sucrose as the carbon source. Sucrose was dissolved in distilled water at a 1.5 M concentration, and the solution was transferred to a Teflon-lined autoclave and heated to 190 °C for 5 h. The resulting slurry was filtered and washed in ethanol. The obtained powder was vacuum-dried at 100 °C for 24 h and annealed at 1000 °C for 2 h under an argon atmosphere. The HCS-S composite was prepared by mixing HCS with sulfur in a 1:5 weight ratio. The mixture was heated at 150 °C for 7 h in a sealed round flask under an argon atmosphere in order to infiltrate the low-viscosity molten sulfur into the HCS pores. Then, the excess sulfur outside the HCS was vaporized by a heat treatment at 300 °C for 2 h. The final sulfur content in the HCS-S composite has been found to be of 42% in weight by meaning of thermogravimetric analysis.

2.2. Lithiated-silicon carbon composite

The spherical nanostructured Si/graphite/carbon composite was synthesized by the following procedure: a pellet of mixed nano-Si/graphite/petroleum pitch powders was heated at 1000 °C under an argon atmosphere. Prior to use in a lithium-ion cell, the silicon-based composite was lithiated by direct contact with a lithium foil in a 1.2 M $LiPF_6$ solution with EC:EMC at a weight ratio of 3:7 for 12 h under 1 kg cm^{-2} pressure.

2.3. Electrolyte

The electrolyte was a solution of lithium trifluoromethane sulfonate, $LiCF_3SO_3$ (Aldrich), in tetraethyleneglycole dimethylether (TEGDME, Aldrich) with a molar ratio of 1:4, prepared in argon-filled glove box.

2.4. Material characterization

The sulfur content in the HCS-S material was determined by thermo-gravimetric analysis (TG 209 F3, Netch) performed in a nitrogen atmosphere with a heating rate of 10 °C min^{-1}. The morphology and crystalline phase were analyzed by field-emission scanning electron microscopy (S-4800, Hitachi), focalized ion beam (KICET instrument), and x-ray diffraction (Rint-2000, Rigaku) with Cu-Kα radiation. The diffraction data were obtained at 2θ = 10–80°, with a step size of 0.03°.

2.5. Electrode preparation and electrochemical tests

The conductivity of the $LiCF_3SO_3$-TEGDME was determined by impedance spectroscopy in a R2032 coin-type cell. The cell included stainless steel-blocking electrodes, and the electrolyte was trapped within a 125-μm-thick Teflon O-ring of 10-mm internal diameter (cell constant k = 0.016 cm^{-1}). The conductivity measurements were performed in a -7–50 °C temperature range with a VMP3 Biologic instrument. The frequency range was 100 Hz–100 kHz, and the voltage amplitude, 30 mV.

The HCS-S electrode was prepared by mixing, in acetonitrile, the active materials with a carbon black conducting agent (acetylene black) and a polyethylene oxide ($M_w = 6 \times 10^5$, Aldrich) binder in a 60:20:20 weight ratio. The resulting slurry was then coated on an Al foil to obtain a film with approximately 40-micron thickness. The electrode was roll-pressed and subsequently dried at 50 °C to remove the residual solvent.

The silicon-based electrode was prepared by mixing, in n-methyl pyrrolidinone, the active material with a carbon black conducting agent (acetylene black) and a carboxymethylcelluose-styrene butadiene rubber (CMC:SBR weight ratio, 1:2) binder in a 85:5:10 weight ratio. The resulting slurry was coated on Cu foil to obtain a film with approximately 30-μm thickness. The electrode was roll-pressed and subsequently dried at 80 °C to remove the residual solvent and then pre-lithiated as reported above.

The single-electrode electrochemical measurements were performed with R2032 coin-type cells. The test electrode was contacted, in an argon-filled glove box, with a lithium foil counter electrode separated by the selected electrolyte solution soaked in a porous polyethylene separator. Full lithium-ion cells were assembled as reported for the single electrode; however, the lithium metal foil was replaced with a pre-lithiated silicon electrode at a mass ratio of 1:1. The response of the single electrode as well as that of the complete cell was tested by galvanostatic cycling at different rates using a TOSCAT-3100 instrument. In the cell, 1C rate (sulfur mass) = 1.68 A $g^{-1}_{(S)}$.

3. Results and discussion

3.1. The cathode

As the cathode of the Si/S battery we have used a sulfur–carbon composite formed by trapping sulfur into highly porous hard carbon spherules (HCSs). The electrode was prepared by the infiltration of molten sulfur in highly porous HCSs. More details are provided in Section 2. The synthetic approach was a refinement of those reported by other workers [12,16,17] in particular similar to that recently reported by Archer and co-workers [12] exploiting important modification that yields a sulfur electrode material with unique characteristics, however with some important differences in the procedure and in the final morphology.

Our electrode material is in fact prepared by using a porous carbon spheres having a high surface area, i.e. 854 m^2 g^{-1} and a very small pore size, i.e. about 1.5 nm, two main features that result

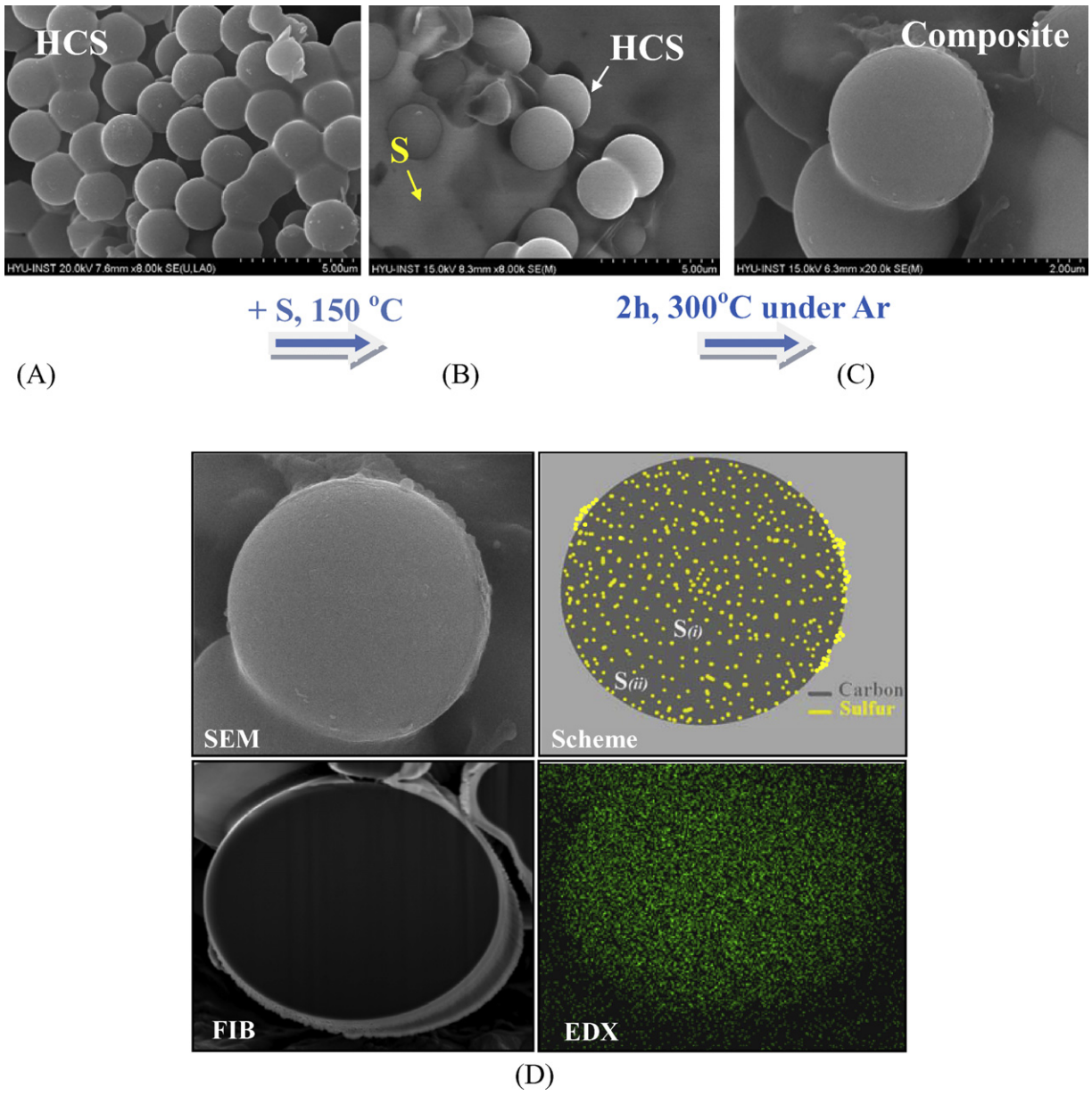

Fig. 1. Scanning electron microscopy (SEM) images of hard carbon spherule-sulfur (HCS-S) electrode taken in the course of its synthesis: (A) the regular shape and the morphology of the pristine HCS particles, (B) the presence of scattered sulfur on the surface of the HCS particles after the first heating step at 150 °C under argon, and (C) the appearance of the final HCS-S composite sample involving the homogeneous dispersion of the sulfur particles in the bulk and over the surface of the HCS particles after vaporization at 300 °C. The top right image in (D) illustrates in scheme the sample morphology and is derived from the SEM image (top left) and the EDX image (bottom right) in which the green spots represent the sulfur on the surface of a HCS-S particle half-split by focused ion beam (bottom left). (For interpretation of the references to color in this figure legend, the reader is referred to the web version of the article.)

in a high tap density, i.e., 1.04 g cm^{-3} and accordingly and more importantly, in a high volumetric energy density of the electrode.

Fig. 1 shows the scanning electron microscopy (SEM) images of our cathode material taken during the course of its synthesis. The images show the regular shape and the morphology of the pristine HCS particles (A), the presence of scattered sulfur on their surface after the first heating step at 150 °C under argon (B), and the appearance of the final HCS-S composite involving the homogeneous dispersion of the sulfur particles in the bulk and over the surface of the HCS particles after the vaporization step at 300 °C (C). This particular morphology is represented by the top-right image shown in Fig. 1D, which was derived from an SEM image (top left) and an energy dispersive x-ray (EDX) image (bottom right) in which the green spots represent the sulfur on the surface of a HCS-S particle half-split by a focused ion beam (FIB) image (bottom left). By contrast, in most conventional HCS-S materials, sulfur is trapped inside the HCS spheres with scarce interparticle distribution [17].

Fig. 2 summarizes the electrochemical properties of the HCS-C composite electrode developed in this work in terms of its cycling response in a lithium cell. Fig. 2A shows that the HCS-S electrode delivers a specific capacity ranging from 1000 mAh g$^{-1}{}_{(S)}$ (i.e., 60% of the 1670 mAh g^{-1} theoretical value of the sulfur) to 650 mAh g$^{-1}{}_{(S)}$ after more than 100 charge–discharge cycles at the very high rate of 1 A g$^{-1}{}_{(S)}$ and 1-V discharge cut-off. We assume that this loss in capacity is associated with a not yet totally blocked polysulfides dissolution. This issue is under study and will be addressed by further optimizing the HCS-S electrode morphology.

The inset of Fig. 2A shows the discharge (formation of lithium sulfide)–charge (reconversion to sulfur) voltage profiles of the cell. All the expected signatures are displayed, namely, two plateaus at

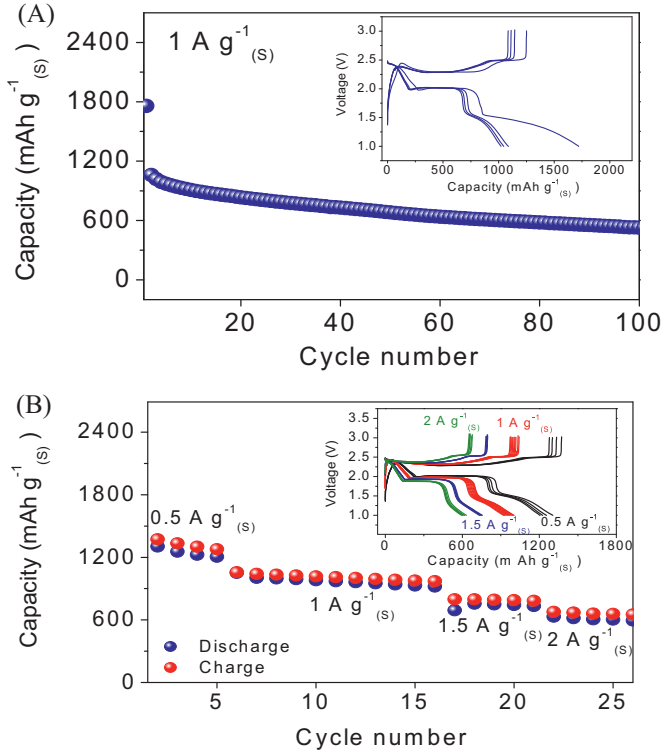

Fig. 2. Capacity versus cycle number and related voltage profiles of the discharge (sulfur conversion in lithium sulfide)–charge (reconversion to sulfur) cycles (inset) for HCS-S electrode in a lithium cell: (A) and (B) at various current rates within 1.0–3.0 V voltage limits. Room temperature. $(TEGDME)_4LiCF_3SO_3$ electrolyte.

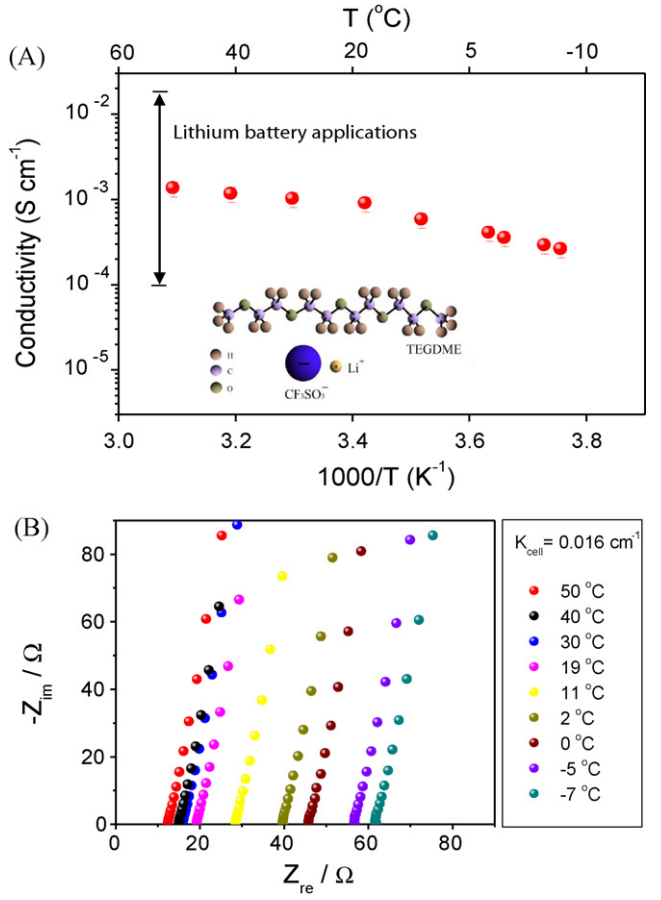

Fig. 3. Transport properties of $(TEGDME)_4LiCF_3SO_3$ electrolyte represented by (A) conductivity Arrhenius plot and (B) impedance spectroscopy Nyquist plot at various temperatures.

2.4 V and 2 V vs. Li, followed by a third one at a lower voltage. We interpret the first two plateaus as associated with the reduction of the sulfur hosted on the surface of the carbon spherules and/or in their inter-particle space (see Fig. 1D) and the third plateau with the reduction of the remaining sulfur inside the particles. Finally, Fig. 2B shows the cycling behavior of the electrode at various current density rates. The steady cycled capacity ranges from 600 mAh $g^{-1}_{(S)}$ at 2 A $g^{-1}_{(S)}$ to 1000 mAh $g^{-1}_{(S)}$ at 0.5 A g^{-1} while maintaining a low charge and discharge voltage gap (see inset of Fig. 2B). These performances make our HCS-C electrode of sure practical interest.

3.2. The electrolyte

The electrolyte used in this work is formed by a solution of lithium triflate, $LiCF_3SO_3$ in tetraethylene glycol dimethyl ether, TEGDME, at the $(TEGDME)_4LiCF_3SO_3$ composition. The general use of glycols as Li/S battery electrolytes has been already proposed in the past [18,19]. The novelty of our material is in its design and composition, involving the use of a very stable lithium salt, i.e., $LiCF_3SO_3$ instead of the common reactive LiTFSI, and in the appropriate ratio of its components. These modifications give an electrolyte having a series of advantages over the most standard organic carbonate electrolytes, including a higher conductivity in a wider temperature range. In addition, the $(TEGDME)_4LiCF_3SO_3$ electrolyte has a high thermal stability (extending up 180 °C), low toxicity and environmental compatibility. As in fact shown by the Arrhenius plot of Fig. 3A, the electrolyte conductivity evolves from 10^{-3} S cm^{-1} to 10^{-4} S cm^{-1} over a temperature range extending from −10 °C to 60 °C, providing the condition necessary for operating the HCS-S electrode even at low temperatures.

3.3. The anode

Clearly, for successful battery application the sulfur cathode requires not only a stable and compatible electrolyte but also its combination with a safe, high-capacity anode. Lithium metal, commonly used in conventional sulfur systems, was excluded due to its reactivity and the associated safety hazard. Our choice was a nanostructured silicon–carbon composite, originally prepared in one of our laboratories [20]. The lithium necessary to assure the electrochemical process was provided by an ex-situ lithiation process by a procedure previously reported [21].

Fig. 4 illustrates the morphological, structural, and electrochemical characteristics of this lithiated silicon–carbon electrode. The SEM image of Fig. 4A reveals that the pristine Si–C composite is formed by micro-sized carbon particles containing the nanostructured silicon. The silicon electrode was prelithiated by using a procedure reported in previous paper [21]. The XRD patterns of Fig. 4B indicate that, after the lithiation, the peaks related to silicon (JCPDS # 75-0590) vanish while new patterns, associated with a partially lithiated silicon phase Li_xSi, does appear. This result demonstrates that our lithiation procedure does not lead to the full $Li_{4.4}Si$ composition, to which is associated a theoretical capacity of 4200 mAh g^{-1}, but to an intermediate phase identified by XRD analysis as $Li_{21}Si_8$ (JCPDS # 33-0817). It is worth to point out that the lithiation was carried out for the purpose of avoiding undesired side reactions at the surface of the Si–C electrode as well as of reaching optimal cell balance. Further work is in progress to fully optimize this procedure with the goal of eliminating

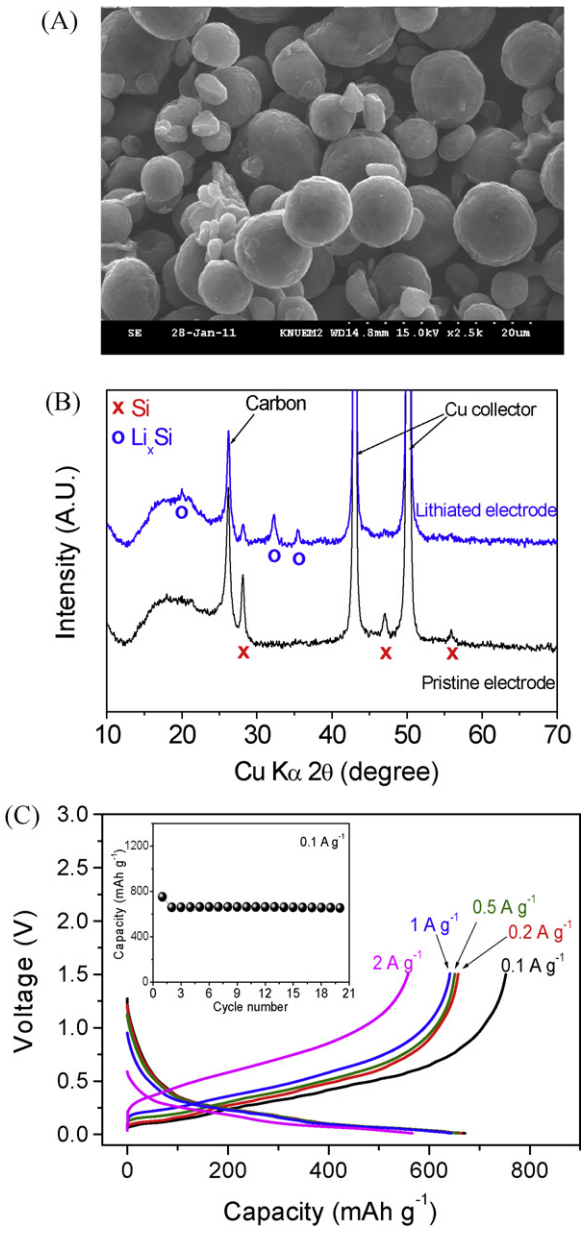

Fig. 4. Morphology, structure, and electrochemical properties of Li_xSi–C: (A) SEM image, (B) XRD patterns before and after pre-lithiation, and (C) voltage profiles of the Li–SiC/Li cell at various current rates and capacity versus cycle number (inset). 100 mA g^{-1} current rate. Room temperature. $(TEGDME)_4LiCF_3SO_3$ electrolyte. Lithium counter electrode.

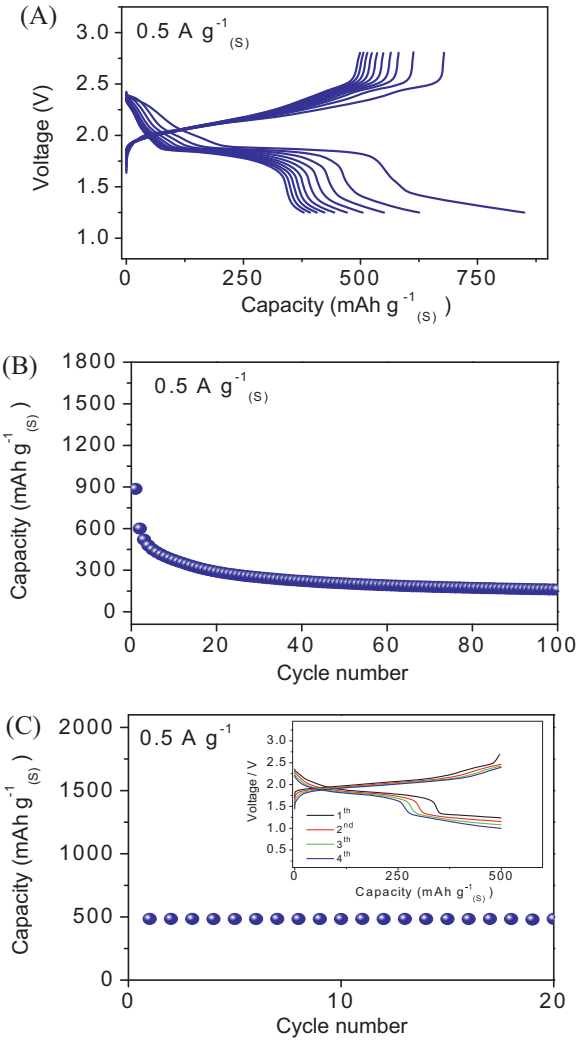

Fig. 5. Cycling behavior of a complete Li_xSi–C/$(TEGDME)_4LiCF_3SO_3$/HCS-S cell: (A) voltage profiles of discharge (de-lithiation at the anode and lithium polysulfides formation at the cathode)–charge (reconversion to sulfur at the cathode and back lithiation at the anode) cycles, (B) capacity versus cycle number at fixed 1.25–2.80 V voltage limits, and (C) capacity versus cycle number and related voltage profiles of discharge–charge cycles (inset) at 1-h fixed time limit. Room temperature. 0.5 A $g^{-1}_{(S)}$ rate. $(TEGDME)_4LiCF_3SO_3$ electrolyte.

completely the irreversible effect of residual electrolyte decomposition processes.

On the basis of this composition and a silicon-to-carbon weight ratio of 30:70, and considering a capacity of 372 mAh g^{-1} for the carbon, we expect for this electrode a specific capacity of the order of 750 mAh g^{-1}, which matches well with the capacity of the HSC-S cathode. Fig. 4C presents the voltage profiles of a Li–Si–C/Li cell using the selected $(TEGDME)_4LiCF_3SO_3$ electrolyte and cycled at various rates. The results demonstrate the good rate capability of the Li–Si–C electrode that can operate at rates as high as 2 A g^{-1}, still maintaining a high capacity delivery. As evident from the inset to the figure, the cell exhibited at 0.1 A g^{-1} a steady specific capacity of the order of 650 mAh g^{-1}, which compares reasonably well with the expected 750 mAh g^{-1} value.

3.4. The silicon–sulfur battery

The above data confirm that the Li–Si–C composite may indeed be a suitable anode for the development of a metal-free, lithium-ion, silicon–sulfur battery. We fabricated the battery by combining this anode, in a 1:1 mass ratio, with the HSC-S cathode in the $(TEGDME)_4LiCF_3SO_3$ electrolyte. The electrochemical performance of this Li–Si–C/HSC-S battery is illustrated in Fig. 5. Fig. 5A shows the voltage profiles from galvanostatic cycling of the cell at room temperature and 0.5 A $g^{-1}_{(S)}$ current rate. The trend confirms that the cell operates with the voltage signatures compatible with the expected electrochemical process $S_8 + 8Li_xSi \leftrightarrows 8Li_2S + 8Li_{(x-2)}Si$ and has an initial capacity approaching 600 mAh $g^{-1}_{(S)}$.

Most of the literature on lithium–sulfur batteries deals with systems where, despite improvements at the cathode side, the use of the lithium metal anode still poses serious risks in terms of safety hazard. Here we show that an important step ahead in the field may be obtained by replacing the lithium metal anode by a high, capacity, lithiated silicon leading to unique example of an efficient, versatile, lithium-ion, silicon–sulfur battery. A sulfur battery using

a silicon-based anode has been proposed in the past [22]; however, it differs significantly from our system since it uses a lithium sulfide–carbon composite cathode and an electrolyte likely formed by a standard organic carbonate liquid, with associated limited performance.

Fig. 5 demonstrates the good performance of our Si–S battery in terms of specific capacity and cycle life. Indeed, even in its not-yet optimized configuration, the silicon–sulfur lithium-ion battery here developed offers impressive cycling performance. Under a galvanostatic cycling regime, the battery delivers a specific capacity of the order of 500 mAh $g^{-1}{}_{(S)}$ at a rate of 0.5 A $g^{-1}{}_{(S)}$ with an average voltage of about 2 V (Fig. 5A). The capacity decreases upon cycling to finally reach an average high value of 300 mAh $g^{-1}{}_{(S)}$ for over 100 cycles (Fig. 5B). An initial irreversible capacity is also noticed. In view of the result of the cycling test reported in Fig. 2A we may reasonably assume that these phenomena are not associated with side reactions occurring at the HSC-S cathode but rather with still unsatisfactory mass balance of the two electrodes. However, also a not yet fully achieved control of the polysulfide dissolution, cannot be excluded. Studies are underway to properly address these remaining issues. We may anticipate that the performance of the battery may be improved by optimizing the cell structure and/or by using ad-hoc protocols, such as time-controlled cycling. Under the latter condition, the capacity remains in fact stable on a set 500 mAh g^{-1} value for many cycles; however, there is an inevitable penalty in terms of voltage stability (Fig. 5C). The data of Fig. 5C lead to a maximum energy density of 1000 Wh kg^{-1}, exceeding the average values achieved by conventional lithium-ion batteries. In addition, by virtue of the nature and the properties of the selected glycol-based electrolyte, the battery is expected to be safe and capable of operating over a wide temperature range. In conclusion, the battery here disclosed, due to the series of properties outlined above, may contribute to the progress of the lithium battery technology in view of application in the electrified road transportation.

Acknowledgements

This work was, in part, performed within the Project “REALIST” (Rechargeable, advanced, nano structured lithium batteries with high energy storage) sponsored by the Italian Institute of Technology (IIT), the World Class University (WCU) program through the National Research Foundation of Korea funded by the Ministry of Education, Science and Technology (R31-2008-000-10092), and the Human Resources Development of the Korea Institute of Energy Technology Evaluation and Planning (KETEP) grant funded by the Korea Government Ministry of Knowledge Economy (No. 20114010203150). The authors wish to thank Mr. Myong Joon Ahn of Kangwon National University, South Korea, for kindly supplying the silicon electrode.

References

[1] M. Armand, J.-M. Tarascon, Nature 451 (2008) 652–657.
[2] X. Ji, L. Nazar, J. Mater. Chem. 20 (2010) 9821–9826.
[3] D. Aurbach, P. Pollak, R. Elasari, G. Salitra, C.S. Kelley, J. Affinito, J. Electrochem. Soc. 156 (2009) A694–A702.
[4] E. Peled, H. Yamin, J. Power Sources 9 (1983) 281–287.
[5] D. Peramunge, S.A. Licht, Science 261 (1993) 1029–1032.
[6] J. Shim, K.A. Stribel, E.J. Cairns, J. Electrochem. Soc. 149 (2002) A1321–A1325.
[7] H.-J. Ahn, K.-W. Kim, J.-H. Ahn, Encycl. Power Sources (2009) 155–161.
[8] S.-E. Cheon, K.-S. Ko, J.-H. Cho, S.-W. Kim, E.-Y. Chin, H.-T. Kim, J. Electrochem. Soc. 150 (2003) A800–A805.
[9] W. Pu, X. He, L. Wang, Z. Tian, C. Jiang, C. Wan, Ionics 13 (2007) 273–276.
[10] X. Ji, K.T. Lee, L.F. Nazar, Nat. Mater. 8 (2009) 500–506.
[11] B. Zhang, Z. Qin, G.R. Lee, X.P. Gao, Energ. Environ. Sci. 3 (2010) 1531.
[12] N. Jayaprakash, J. Shin, S.A. Moganty, A. Corona, L.A. Archer, Angew.Chem. Int. Ed. 50 (2011) 5904–5908.
[13] X. Ji, S. Evers, R. Black, L.F. Nazar, Nat. Comm. 2 (2011) 325.
[14] J. Hassoun, B. Scrosati, Angew. Chem. Int. Ed. 49 (2010) 2371–2374.
[15] J. Hassoun, B. Scrosati, Adv. Mater. 22 (2010) 5198–5201.
[16] C. Lai, X.P. Gao, B. Zhang, T.Y. Yan, Z. Zhou, J. Phys. Chem. C 113 (2009) 4712–4716.
[17] B. Zhang, X. Qin, G.R. Li, X.P. Gao, Energy Environ. Sci. 3 (2010) 1531–1537.
[18] Song, et al., J. Electrochem. Soc. 151 (2004) A791–A795.
[19] C. Liang, N.J. Dudney, J.Y. Howe, Chem. Mater. 21 (2009) 4724–4730.
[20] J.-H. Lee, W.-J. Kim, J.-Y. Kim, S.-H. Lim, S.-M. Lee, J. Power Sources 176 (2008) 353–358.
[21] J. Hassoun, K.-S. Lee, Y.-K. Sun, B. Scrosati, J. Am. Chem. Soc. 133 (2011) 3139–3143.
[22] Y. Yang, M.T. McDowell, A. Jackson, J.J. Cha, S.S. Hong, Y. Cui, Nano Lett. 10 (2010) 1486–1491.